Journal of Solid State Chemistry **144,** 372–378 (1999)
Article ID jssc.1999.8168, available online at http://www.idealibrary.com on IDEAL®

A Powder Neutron Diffraction Study of the Magnetic Structure of FeV_2S_4

Anthony V. Powell,*,[1] Clemens Ritter,† and Paz Vaqueiro*

*Department of Chemistry, Heriot–Watt University, Riccarton, Edinburgh EH14 4AS, United Kingdom; and †Institut Max von Laue–Paul Langevin, F-38042 Grenoble, France

Received October 5, 1998; in revised form January 13, 1999; accepted January 18, 1999

Variable-temperature powder neutron diffraction data demonstrate that FeV_2S_4 undergoes a transition to a long-range magnetically ordered state at 135(7) K, in agreement with magnetic susceptibility data. High-resolution neutron diffraction data collected at 1.9 K reveal that magnetic ordering results in a doubling of the crystallographic unit-cell dimensions ($I2/m$ $a = 5.8302(2)$, $b = 3.2761(1)$, $c = 11.2398(4)$ Å, $\beta = 92.046(2)^\circ$) in the a and c directions and that the magnetic structure is described by a propagation vector of $(\frac{1}{2}, 0, \frac{1}{2})$. Cations in an ordered defect layer, 76% of which are Fe(II), possess an average ordered moment of 1.86(5) μ_B, which is directed at an angle of 75° to the layer. Cation–cation interactions reduce the average moment of cations in the MS_2 unit to 0.17(4) μ_B. The complex magnetic structure involves essentially collinear antiferromagnetic ordering between nearest-neighbor cations. © 1999 Academic Press

INTRODUCTION

Many transition metal sulfides adopt low-dimensional or pseudo-low-dimensional structures as a consequence of the high polarizability and covalency of the sulfide anion (1). This is exemplified by the layered structures of the transition metal dichalcogenides, which consist of MS_2 units formed from either edge-linked MS_6 octahedra or MS_6 trigonal prisms, separated by a van der Waals gap. The MS_2 unit can also be considered as the building block for a variety of three-dimensional structures. In particular, occupation of a fraction of the vacant octahedral sites between pairs of disulfide units containing edge-linked octahedra results in a range of structures between the cadmium iodide (MS_2) and nickel arsenide (MS) structures (2). At 50% occupancy, ordering of defects gives rise to the $\sqrt{3}a_p \times a_p$ superstructure (where a_p refers to the primitive hexagonal unit cell of the nickel arsenide structure) of the Cr_3S_4 structure (3) (Fig. 1). In addition to several binary chalcogenides, many ternary phases of stoichiometry AM_2S_4 (A = V, Cr, Fe, Co, Ni; M = Ti, V, Cr) adopt this structure (4) for which two limiting cation distributions can be envisaged. If sites in the vacancy layer are exclusively occupied by the A cation, the arrangement is termed the normal structure, whereas the inverse structure corresponds to occupation of such sites solely by the M cation. However, partitioning of cations between the octahedral sites in the MS_2 unit and those in the ordered defect layer is often incomplete and depends on the relative positions of the cations in the transition series (5–7).

During a recent study (8) of a series of isostructural Cr_3S_4-type sulfides, AV_2S_4 (A = Ti, Cr, Fe, Ni), it was shown that both cation site preferences and physical properties are sensitive to the nature of the A cation. A combination of powder X-ray and neutron diffraction revealed a progressive structural change from a near inverse structure in TiV_2S_4 to a near normal structure for NiV_2S_4. The chromium and iron analogues adopt intermediate structures in which the A cation is distributed between the two octahedral sites. Although other workers have interpreted magnetic susceptibility (9), Mössbauer (10, 11) and neutron diffraction data (12) for FeV_2S_4 on the basis of a single iron site, Rietveld analysis using X-ray and neutron data simultaneously, reveals that ca. 25% of the iron resides in the fully occupied layer. This is in excellent agreement with the results of an earlier neutron diffraction study (7).

All materials, with the exception of semiconducting CrV_2S_4, are metallic. However, magnetic properties show greater variation. When the A cation is drawn from the early part of the transition series, there is little evidence for long-range magnetic order: TiV_2S_4 is paramagnetic while CrV_2S_4 is a spin-glass. Magnetic susceptibility data for NiV_2S_4 exhibit relatively little temperature dependence and are of a form similar to those of $NiCr_2S_4$ (13), suggesting similar bulk magnetic properties. In contrast, several workers (8–10, 14–15) have reported that magnetic susceptibility data for FeV_2S_4 exhibit a well-defined maximum at 131–145 K. The absence of any divergence between zero-field-cooled

[1]To whom crrespondence should be addressed. E-mail: A.V.Powell@hw.ac.uk.

0022-4596/99 $30.00

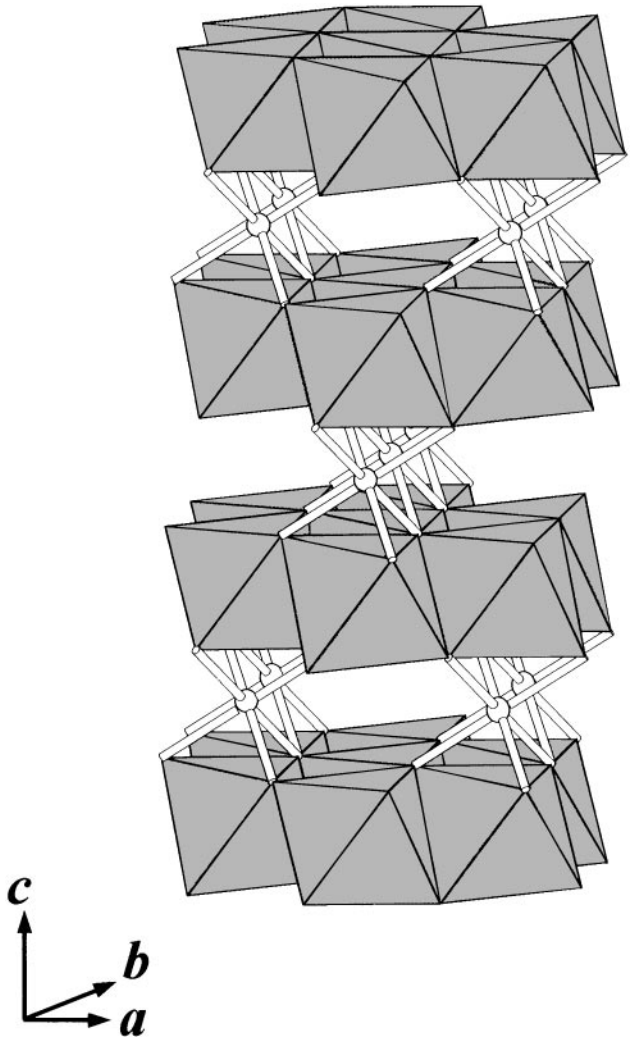

FIG. 1. The Cr_3S_4 structure. Cations in the ordered defect layer are shown as solid circles and cations in the fully occupied layer lie at the center of shaded MS_6 octahedra which share edges to form a layer of stoichiometry MS_2.

and field-cooled susceptibilities at this temperature (Fig. 2) suggests that this corresponds to a transition to a long-range magnetically ordered state. While time-of-flight powder neutron diffraction data collected at 4.2 K have confirmed the presence of long-range magnetic order at low temperatures (8), attempts to determine the magnetic structure of FeV_2S_4 were unsuccessful. This was a consequence of the small number of magnetic Bragg peaks present in the data and the relatively poor resolution at long d spacings on an energy dispersive instrument. In seeking to resolve this problem, high-resolution powder neutron diffraction data have been collected in angle dispersive mode. These have permitted the determination of the magnetic structure of FeV_2S_4, which differs from that previously observed for related ternary chromium sulfides of the Cr_3S_4 type.

EXPERIMENTAL

The sample of FeV_2S_4 used in this work had been prepared by reaction of the powdered elements at 1023 K in an evacuated, sealed silica ampoule during the course of an earlier investigation of cation ordering in ternary vanadium sulfides. A combination of powder X-ray diffraction, thermogravimetry, and energy dispersive X-ray microanalysis confirmed the material to be a single phase of composition $Fe_{0.99}V_{2.01}S_{3.96}$. Full details of the preparation and characterization have been presented elsewhere (8).

High-resolution powder neutron diffraction data were collected at 1.9 K over the angular range $0 \leq 2\theta/^\circ \leq 160$ at a neutron wavelength of 1.590 Å on the D2B diffractometer at the high-flux reactor, ILL, Grenoble. Approximately 3 g of sample were contained in a thin-walled vanadium can, mounted in a standard ILL cryostat, and data were collected over a period of ca. 5 h. Variable temperature measurements were made on the high intensity diffractometer D1B, also at ILL, over the angular range $20 \leq 2\theta/^\circ \leq 100$ using a neutron wavelength of 2.524 Å. Data were collected over the temperature range $1.3 \leq T/\mathrm{K} \leq 166$ in increments of ca. 15 K, counting for 10 min at each temperature. Rietveld refinements were carried out using the GSAS (16) package installed on the Heriot-Watt University Alpha 2100-4275 system.

RESULTS

In addition to reflections arising from the nuclear structure, several low-angle peaks, the most intense of which occur at $2\theta \approx 14.2, 23.7, 31.7^\circ$, were apparent in the high-resolution D2B data. These could be indexed on the basis of an enlarged unit cell consistent with a doubling of the

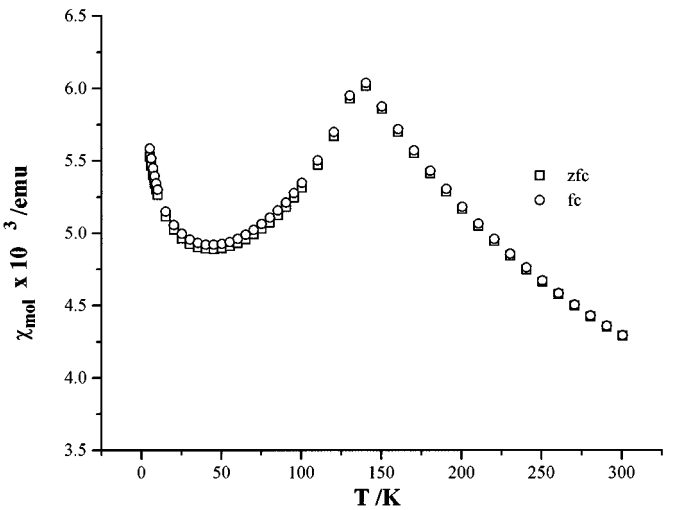

FIG. 2. Zero-field cooled (zfc) and field cooled (fc) molar magnetic susceptibilities for FeV_2S_4 measured in a field of 1000G.

crystallographic unit-cell in the a and c directions, similar to that observed for $NiCr_2S_4$ (13). The crystallographic structure, obtained using a combination of powder X-ray diffraction and time-of-flight powder neutron diffraction at 298 K (8), in which only ca. 12% of sites in the MS_2 unit are occupied by iron, was used for the initial model of the nuclear structure at 1.9 K. Neutron scattering lengths incorporated within GSAS were used. The background was fitted using a cosine Fourier series, with the coefficients included as refinable parameters, and peak profiles were modeled using a pseudo-Voigt function. High-angle data, in which no contributions from magnetic scattering were observed, were used to refine the instrumental, lattice, and positional parameters at 1.9 K. Initially, a trial magnetic structure for FeV_2S_4, described in space group $P1$, was derived from that of $NiCr_2S_4$. The angular dependence of the magnetic scattering was described using the free-ion form factors (17) for Fe^{2+} and V^{3+}. The average scattering from each of the two crystallographically independent sites was approximated by the form factor of the majority cation at each site, although refinement appeared to be relatively insensitive to the choice of from factor used to describe the scattering from a particular site. Only magnetic scattering below $2\theta = 60^\circ$ was included in the refinement. The agreement between observed and calculated data in the regions of the magnetic reflections was poor and did not improve significantly following refinement of magnetic vector components. Therefore, despite a similarly enlarged magnetic unit cell, the magnetic structure of FeV_2S_4 differs from that of $NiCr_2S_4$ and Cr_3S_4. Close examination of the profile revealed that the feature at $2\theta \approx 14.1^\circ$ coincides with the (1/2, 0, −3/2) magnetic reflection (where the indices refer to the crystallographic unit cell) for which the calculated intensity is low for this model. Conversely, the (1/2, 0, 3/2) reflection at $2\theta \approx 14.7^\circ$, has an appreciable calculated intensity, although little intensity is measured in this region.

During a study of magnetic ordering in binary Cr_3X_4 chalcogenides, Bertaut *et al.* (18) derived the possible magnetic configurations for isotropic exchange. Of the four arrangements which result, two correspond to a propagation vector $(\frac{1}{2}, 0, -\frac{1}{2})$ for which (1/2, 0, 3/2) is a permitted magnetic reflection. The magnetic structures of Cr_3X_4 (X = S, Se) and $NiCr_2S_4$ correspond to the member of this pair in which there is antiferromagnetic exchange between cations at each of the two sites. The other pair of configurations correspond to a propagation vector of $(\frac{1}{2}, 0, \frac{1}{2})$ and it is the (1/2, 0, −3/2) magnetic reflection which is allowed. Hence, the powder neutron diffraction data presented here reveal that the magnetic structure of FeV_2S_4 is described by a propagation vector different from that of the related chromium sulfides. Of the two possibilities labeled A and B in the original analysis of Bertaut *et al.*, it is the former in which there is antiferromagnetic exchange between cations in the two crystallographic sites. Therefore, a second trial magnetic structure, in space group $P1$, was constructed using this configuration. Initially, only z components of the two cation moments were considered and their magnitudes refined. On introduction of the remaining magnetic vector

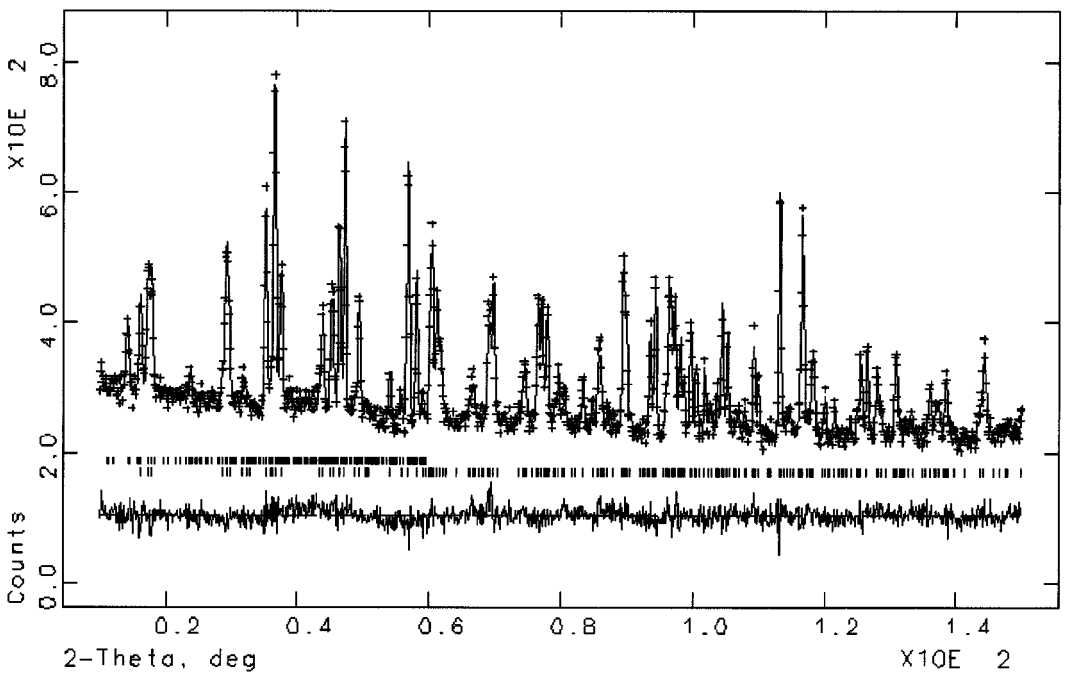

FIG. 3. Final observed (crosses), calculated (full line), and difference (lower full line) neutron profiles for FeV_2S_4 at 1.9 K. Reflection positions are marked: the lower markers refer to the crystallographic unit-cell and the upper markers the magnetic unit-cell described in the primitive space group $P1$.

components, the μ_x component alone of the vacancy layer moment showed any significant deviation from zero: the remaining magnetic vector components were therefore fixed at zero. It should be noted however that refinements of similar quality were obtained when the moment in the fully occupied layer was constrained to lie parallel to the layer direction. Therefore, although refinements indicate the existence of a small moment on the cations in this layer, its direction cannot be considered to be well defined. The final cycles of refinement involved 21 variables and resulted in a weighted residual of 4% and the observed, calculated, and difference profiles of Fig. 3. Refined structural and derived parameters corresponding to the magnetic structure shown in Fig. 4 appear in Table 1.

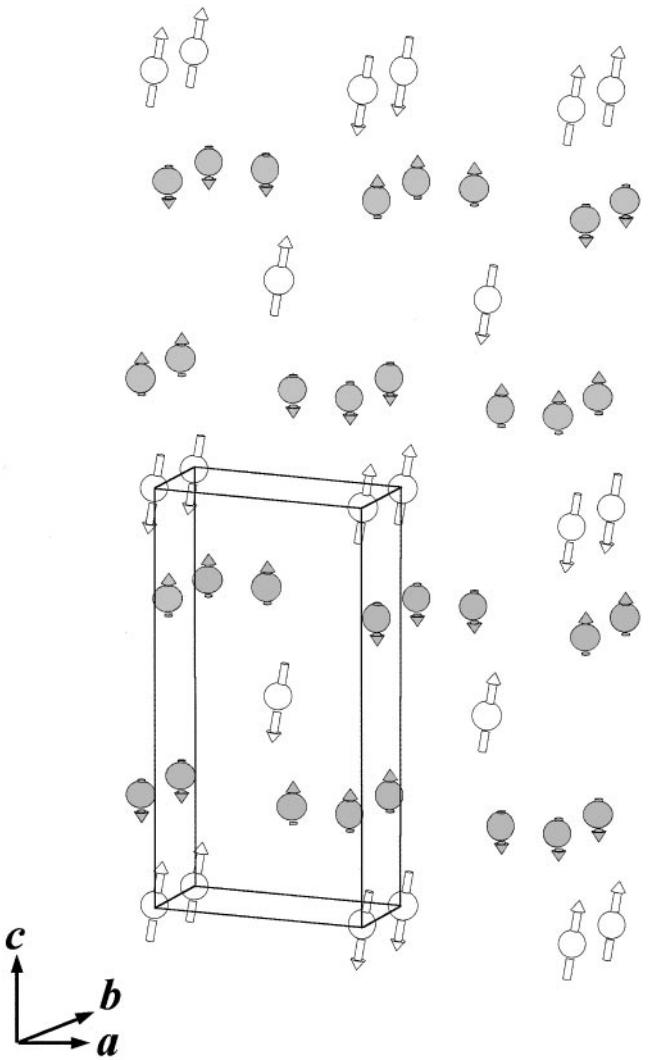

FIG. 4. A representation of the magnetic structure of FeV_2S_4. Sulfide ions are omitted for clarity. Shaded arrows represent moments in the fully occupied layer and open arrows represent moments in the ordered defect layer. The crystallographic unit cell is outlined.

The same model applied to data collected on D1B at 1.3 K resulted, after refinement of a scale factor, background and peak shape parameters, in a low-weighted residual. Thermal parameters derived from D1B data have been found to be unreliable (13) owing to the limited Q range of the data and were therefore fixed at the values determined from high-resolution data while the remaining lattice, positional, and magnetic moment parameters were refined. Refined moments were within a standard deviation of the values reported in Table 1. Powder neutron diffraction data in the angular range $20 \leq 2\theta/^\circ \leq 50$, collected at temperatures between 1.3 and 166 K are plotted in Fig. 5, in which the thermal evolution of magnetic reflections may be observed. The magnetic ordering temperature was determined as 135(7) from a plot of the intensity as a function of temperature of the strong (1/2, 0, $-3/2$) reflection, which with this wavelength appears at $2\theta \approx 22.5^\circ$ (Fig. 5). Sequential Rietveld refinement performed on data collected at higher temperatures demonstrated that unit-cell parameters show little temperature dependence, increasing by $< 0.2\%$, and that there are no marked anomalies at the magnetic ordering temperature. In contrast with members of the $Ni_xCr_{3-x}S_4$ ($0 \leq x \leq 1$) series (19), which exhibit an increase in the monoclinic angle on cooling, β is effectively constant over the entire temperature range in FeV_2S_4. The temperature variation of the ordered magnetic moment at each of the two cation sites was also obtained from sequential Rietveld refinement (Fig. 6).

DISCUSSION

Powder neutron diffraction data demonstrate that FeV_2S_4 undergoes a transition to a magnetically ordered state at 135 K, the temperature at which the maximum magnetic susceptibility is observed. This is significantly lower than ordering temperatures in the $Ni_xCr_{3-x}S_4$ series, which range from 220 K in the binary chromium sulfide ($x = 0.0$) (21) to 180 K in the stoichiometric ternary material ($x = 1.0$) (13). This suggests that interactions involving V(III) are weaker than those involving Cr(III). Below the ordering temperature, the low residual moment in the fully occupied layer shows very little temperature dependence, whereas that associated with the predominantly Fe(II) cations in the ordered defect layer increases on cooling, reaching an apparently limiting value at ca. 30 K.

The magnetic structure of FeV_2S_4 consists of planes, parallel to the (101) crystallographic planes, of ferromagnetically coupled Fe(II) ions within an effectively non magnetic vanadium sulfide matrix. Successive planes of Fe(II) ions are antiferromagnetically aligned with respect to each other. This arrangement differs from that of related chromium sulfides ACr_2S_4 (A = Cr, Ni) (13, 18, 21), which may be described in terms of ferromagnetic sheets parallel to the $(10\bar{1})$ planes antiferromagnetically coupled to each other.

TABLE 1
Refined Parameters for FeV_2S_4 Obtained from High-Resolution Data Collected at 1.9 K

Space group: $I2/m$; $a = 5.8302(2)$, $b = 3.2761(1)$, $c = 11.2398(4)$ Å, $\beta = 92.046(2)^\circ$

						Magnetic vector components			
Atom	Site	x	y	z	B/Å^2	M_x	M_y	M_z	Moment/μ_B
$(M)^a$	2(*a*)	0.0	0.0	0.0	0.51(4)	0.57(8)	0.0	1.77(7)	1.86(5)
$[M]^b$	4(i)	− 0.065(2)	0.0	0.2619(8)	0.51(4)	0.0	0.0	0.17(4)	0.17(4)
S(1)	4(i)	0.3372(5)	0.0	0.3608(3)	0.24(4)				
S(2)	4(i)	0.3376(5)	0.0	0.8894(2)	0.29(4)				

$R_{wp} = 4.0\%$ $\chi^2 = 1.4$
[a] (M): 75.8% Fe; 24.2% V.
[b] $[M]$: 12.1% Fe; 87.9% V.

Ordered moments at each of the two crystallographic sites in ACr_2S_4 are reduced from their spin-only values by the effects of covalency. It has been proposed (22) that FeV_2S_4 contains exclusively high-spin Fe(II), which was assumed to be located at a single site. The reduction of the vacancy layer moment to ca. 50% of the weighted average of spin-only values for localized Fe(II) and V(III) moments is similar to that observed in $NiCr_2S_4$. Although data for related phases (10, 23) suggest that iron in the fully occupied layer may be present as low-spin Fe(II), which would not carry a moment, the moment in this layer is considerably smaller than that expected for V(III) cations reduced by the effects of covalency alone. Similarly, low moments have been observed in several structurally related chalcogenides (24–26), including a moment of 0.14 μ_B in Cr_2Te_3 (27) and indicate that a localized electron description is inapplicable. Delocalization of electrons associated with vanadium cations in materials containing the VS_2 structural unit has been suggested by several workers. Magnetic susceptibility and NMR investigations of V_3S_4 and the structurally related V_5S_8 led de Vries and Haas (28) to conclude that the electrons associated with the vanadium cations located in the VS_2 unit are itinerant and do not contribute a temperature dependent term to the susceptibility. This is in agreement with the results of Nozaki *et al.* who have shown that the high-temperature effective magnetic moment in V_5S_8 arises solely from vanadium cations in the ordered vacancy layer (29). Furthermore, at low temperatures, in the magnetically ordered state, only the vacancy layer cations possess an ordered moment (30). Similarly, Murugesan *et al.* (14) have suggested that vanadium electrons are delocalized in A_xVS_2 (A = Fe, Co, Ni, $x = \frac{1}{4}, \frac{1}{2}$). These observations indicate that electrons reside in narrow bands. This is consistent with the suggestion of Holt *et al.* (31) that the delocalized nature of the electrons associated with the VS_2 unit arises from the formation of a narrow band derived from direct overlap of cation t_{2g} orbitals which, for a formal oxidation state of V(III):d^2, is incompletely filled. Substitution of ca. 12% of

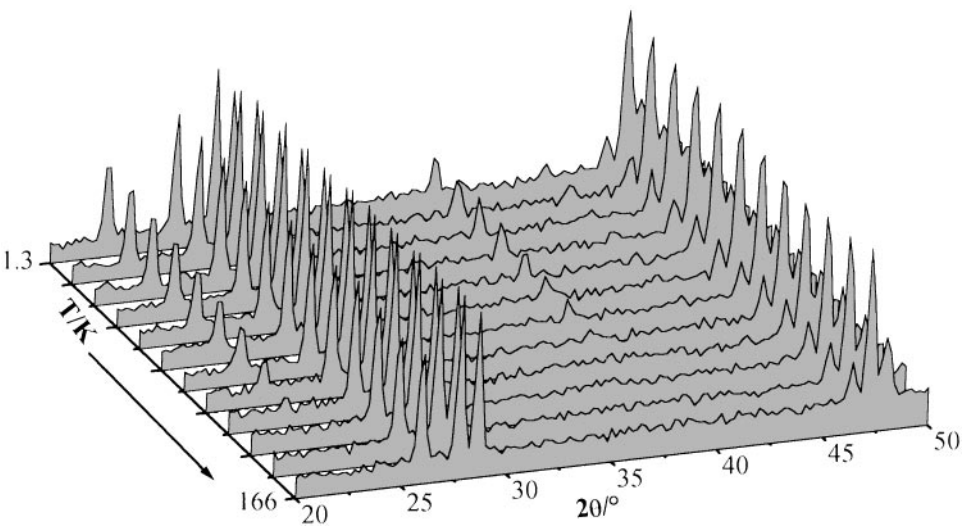

FIG. 5. Powder neutron diffraction data for FeV_2S_4 over the temperature range $1.3 \leq T \leq 166$ K.

TABLE 2
Bond Lengths (Å) and Bond Angles (°) in FeV_2S_4 at 1.9 K

Bond		Angle	
(*M*)–S(1)	2.435(2) × 4	S(1)–(*M*)–S(1)	84.57(9) × 2
(*M*)–S(2)	2.366(3) × 2		95.43 (9) × 2
mean (*M*)–S	2.41	S(1)–(*M*)–S(2)	88.55(8) × 4
			91.45 (8) × 4
[*M*]–S(1)	2.561(9)	S(1)–[*M*]–S(1)	75.3(2) × 2
	2.546(7) × 2		80.1(3)
[*M*]–S(2)	2.284(9)	S(1)–[*M*]–S(2)	88.3(3) × 2
	2.262(6) × 2		87.7(3) × 2
mean [*M*]–S	2.41		91.39(9) × 2
		S(2)–[*M*]–S(2)	106.8(3) × 2
(*M*)–[*M*]	2.981(9) × 2		92.8(3)
[*M*]–[*M*]	2.71(1) × 2		
	4.04(2) × 2		

V(III) in the MS_2 unit by Fe(II) although raising the Fermi level would not produce a filled band. This would account for the experimentally observed metallic behavior and large temperature independent contribution to the magnetic susceptibility (8).

The magnetic structure of the ACr_2S_4 (A = Ni, Cr) phases has been analyzed in terms of individual superexchange interactions (13, 21, 32) by application of the qualitative coupling rules developed by Goodenough (33) and Kanamori (34). Consideration of the relative strengths of competing direct cation–cation interactions and 90° correlation superexchange interactions correctly predicts the presence of both ferromagnetic and antiferromagnetic exchange within the fully occupied layer and antiferromagnetic coupling between cations in different layers. The geometry of the fully occupied layer in FeV_2S_4 differs from that of the chromium analogues. In the Cr_3S_4 structure, each cation in the fully occupied layer has two in-plane neighbors arising from lattice translations of $\pm b$. In FeV_2S_4, these two neighbors are at a slightly shorter distance than in ACr_2S_4 (A = Cr, Ni). In addition, there are two pairs of cations within the same layer, at 4.04 and 2.7 Å. The ratio of these distances is markedly greater than that determined for Cr_3S_4 and $NiCr_2S_4$ (1.16 and 1.14, respectively). This, together with the delocalized nature of the electrons in the fully-occupied layer, appears to be sufficient to reverse the signs of the interactions between those cations in the fully occupied layer which are not related by a lattice translation along b.

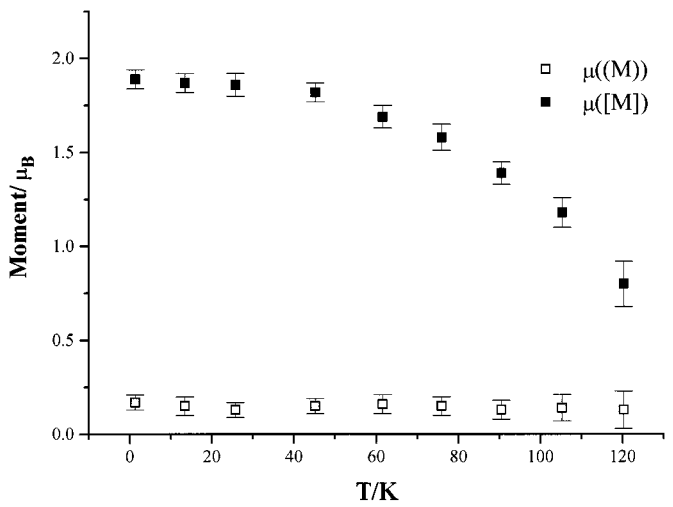

FIG. 6. The temperature dependence of the ordered moments associated with cations at sites in the vacancy (*M*) and fully-occupied [*M*] layers in FeV_2S_4.

ACKNOWLEDGMENT

The authors thank The Leverhulme Trust for a research fellowship for P.V.

REFERENCES

1. C. N. R. Rao and K. P. R. Pisharody, *Prog. Solid State Chem.* **10,** 207 (1979).
2. F. Hulliger, *Struct. Bonding* **4,** 83 (1968).
3. F. Jellinek, *Acta. Crystallogr.* **10,** 620 (1957).
4. A. Wold and K. Dwight, *in* "Solid State Chemistry: Synthesis, Structure and Properties of Selected Oxides and Sulfides," Chapter 11. Chapman and Hall, New York, 1993.
5. D. C. Colgan and A. V. Powell, *J. Mater. Chem.* **6,** 1579 (1996).
6. D. C. Colgan and A. V. Powell, *J. Mater. Chem.* **7,** 2433 (1997).
7. J. M. Newsam and Y. Endoh, *J. Phys. Chem. Solids* **48,** 607 (1987).
8. A. V. Powell, D. C. Colgan, and P. Vaqueiro, *J. Mater. Chem.* **9,** 485 (1999).
9. H. Nozaki and H. Wada, *J. Solid State Chem.* **47,** 69 (1983).
10. Y. Oka, K. Kosuge, and S. Kachi, *Mater. Res. Bull.* **12,** 1117 (1977).
11. H. Nozaki, H. Wada, and H. Yamamura, *Solid State Commun.* **44,** 63 (1982).
12. I. Kawada and H. Wada, *Physica B* **105,** 223 (1981).
13. A. V. Powell, D. C. Colgan, and C. Ritter, *J. Solid State Chem.* **134,** 110 (1997).
14. T. Murugesan, S. Ramesh, J. Gopalakrishnan, and C. N. R. Rao, *J. Solid State Chem.* **44,** 119 (1982).
15. B. L. Morris, R. H. Plovnick, and A. Wold, *Solid State Commun.* **7,** 291 (1969).
16. A. C. Larson and R. B. von Dreele, "General Structure Analysis System," Los Alamos Laboratory Report, LAUR 86-748, 1994.
17. P. J. Brown *in* "International Tables for Crystallography, Vol. C" (A. J. C. Wilson, Ed.), Chap. 4. Kluwer, Dordrecht, 1992.
18. E. F. Bertaut, G. Roult, R. Aleonard, R. Pauthenet, M. Chevreton, and R. Jansen, *J. Phys.* (*Paris*) **25,** 582 (1964).
19. A. V. Powell, D. C. Colgan, and C. Ritter, *J. Solid State Chem.* **143,** 163 (1999).
20. D. Babot, M. Chevreton, J. L. Buevoz, R. Langier, B. Lambert-Andron, and M. Wintenberger, *Solid State Commun.* **30,** 253 (1979).
21. B. Andron and E. F. Bertaut, *J. Phys.* (*Paris*) **27,** 619 (1966).

22. S. Muranaka and T. Takada, *J. Solid State Chem.* **14,** 291 (1975).
23. F. J. Disalvo, M. Eibschütz, C. Cros, D. W. Murphy, and J. W. Waszcak, *Phys. Rev. B* **19,** 3441 (1979).
24. T. J. A. Popma, C. Haas, and B. van Laar, *J. Phys. Chem. Solids* **32,** 581 (1971).
25. B. van Laar, *Phys. Rev.* **156,** 654 (1967).
26. A. F. Andresen, *Acta. Chem. Scand.* **22,** 827 (1968).
27. T. Hamasaki, T. Hashimoto, Y. Yamaguchi, and H. Watanabe, *Solid State Commun.* **16,** 895 (1975).
28. A. B. De Vries and C. Haas, *J. Phys. Chem. Solids* **34,** 651 (1973).
29. H. Nozaki, M. Umehara, Y. Ishizawa, M. Saeki, T. Mizoguchi, and M. Nakahira, *J. Phys. Chem. Solids* **39,** 851 (1978).
30. S. Funahashi, H. Nozaki, and I. Kawada, *J. Phys. Chem. Solids* **42,** 1009 (1981).
31. S. L. Holt, R. J. Bouchard, and A. Wold, *J. Phys. Chem. Solids* **27,** 755 (1966).
32. A. V. Powell and S. Oestreich, *J. Mater. Chem.* **6,** 807 (1996).
33. J. B. Goodenough, "Magnetism and the Chemical Bond." Wiley, New York, 1963.
34. J. Kanamori, *J. Phys. Chem. Solids*, **10,** 87 (1959).